

AperTO - Archivio Istituzionale Open Access dell'Università di Torino

Factors Ruling the Uptake of Silica Nanoparticles by Mesenchymal Stem Cells: Agglomeration Versus Dispersions, Absence Versus Presence of Serum Proteins

This is the author's manuscript

Original Citation:

Availability:

This version is available <http://hdl.handle.net/2318/1521210> since 2017-06-27T17:07:35Z

Published version:

DOI:10.1002/sml.201400698

Terms of use:

Open Access

Anyone can freely access the full text of works made available as "Open Access". Works made available under a Creative Commons license can be used according to the terms and conditions of said license. Use of all other works requires consent of the right holder (author or publisher) if not exempted from copyright protection by the applicable law.

(Article begins on next page)



UNIVERSITÀ DEGLI STUDI DI TORINO

This is an author version of the contribution published on:

Questa è la versione dell'autore dell'opera:

Small, 11 (24), 2015, DOI: 10.1002/sml.201400698

The definitive version is available at:

La versione definitiva è disponibile alla URL:

<http://www.interscience.wiley.com/>

Article type: Full Paper

Factors Ruling the Uptake of Silica Nanoparticles by Mesenchymal Stem Cells: Agglomeration vs Dispersions, Absence vs Presence of Serum Proteins

*Federico Catalano, Lisa Accomasso, Gabriele Alberto, Clara Gallina, Stefania Raimondo, Stefano Geuna, Claudia Giachino and Gianmario Martra**

[*] Dr. F. Catalano, Dr. G. Alberto, Prof. G. Martra

Department of Chemistry and Interdepartmental Centre of Excellence “Nanostructured Interfaces and Surfaces – NIS”, University of Turin, Via P. Giuria 7, 10125 Torino, Italy
Email: gianmario.martra@unito.it

Dr. L. Accomasso, Dr. C. Gallina, Dr. S. Raimondo, Prof. S. Geuna, Prof. C. Giachino
Department of Clinical and Biological Sciences, University of Turin, Regione Gonzole 10, 10043 Orbassano (Torino), Italy

Keywords: silica nanoparticles, dispersion, serum protein adsorption, uptake by mesenchymal stem cells

Abstract:

The results of a systematic investigation of the role of serum proteins on the interaction of silica nanoparticles (NP) doped in their bulk with fluorescent molecules (IRIS Dots, 50 nm in size), with human mesenchymal stem cells (hMSCs) are reported. The suspension of IRIS Dots in bare Dulbecco-Modified Eagle’s Medium (DMEM) results in the formation of large agglomerates (ca. 1.5 μm , by dynamic light scattering), which become progressively smaller, down to ca. 300 nm in size, by progressively increasing the fetal bovine serum (FBS) content of the solutions along the series 1.0, 2.5, 6.0 and 10.0% v/v. Such difference in NP dispersion is maintained in the external cellular microenvironment, as observed by confocal microscopy and transmission electron microscopy. As a consequence of the limited diffusion of proteins in the inter-NP spaces, the surface of NP agglomerates is coated by a protein corona independently of the agglomerate size/FBS concentration conditions (ζ -potential and UV circular dichroism measurements). The protein corona appears not to be particularly relevant for the uptake of IRIS Dots by hMSCs, whereas the main role in determining the internalization rate is played by the absence/presence of serum proteins in the extra-cellular media.

1. Introduction

“What the cells see”^[1] is the question that in present days researchers are asking themselves when investigating the response elicited in complex biological media (cell cultures or tissues) by nanoparticles (NP). Indeed, such response is the result of the actual state of the exogenous materials, typically in terms of the layers of adsorbed proteins (the so called “corona”), responsible for the interaction with cell membrane and receptors.^[2-6] In this concern, several studies have reported that the protein corona, obtained from incubation in 10% v/v fetal bovine serum (FBS), reduces the adhesion of NP to cell membrane, leading to reduced cellular uptake.^[7,8] However, also the dispersion state should play a significant role.^[9] In several cases preparation methods have been finely tuned to obtain stable suspension of monodispersed NP, but suspension media and conditions can be significantly different with respect to the incubation and/or pre-incubation media used for *in vitro* or *in vivo* studies. For instance, on one hand the presence of divalent cations (typically Ca^{2+} and Mg^{2+}) can affect in a significant extent the surface potential of negatively charged surfaces (as usually those of NP at physiological pH), leading to a substantial decrease in the repulsive double-layer forces between surfaces.^[10] On the other hand, adsorbed protein can act as surfactants, and the final dispersion state of NP in experimental conditions should result from a complex balance between different effects. In such a scenario, it is worth to notice that different protocols for *in vitro* cell tests can require different concentration of proteins in the culture medium.^[11-13] Hence, discrepancies among results obtained in such tests might also depend on difference in the interplay among the factors indicated above. Moreover, the rationalisation of these effects on the basis of *in vitro* experiments could allow to attain some insight also useful for the analysis of data obtained *in vivo*.

Flourishing research activities in the field of nanoscience are exploring and demonstrating the possibility of exploiting in life science smart properties of different classes of nanoparticles, both organic and inorganic in nature, as well as of their composites and hybrids.^[14] Among

the hybrid ones are fluorescent dyes-silica nanoparticles which, by suitably pairing dyes and preparation methods can exhibit a very intense photoluminescence,^[15] and then behave as highly effective optical nanotools.^[16] In this concern, IRIS Dots are fluorescent hybrid dye-silica NP developed in our laboratory for the attempt of optical imaging.^[17,18] As we showed in a previous work, IRIS Dots are suitable for efficient and harmless long-term human Mesenchymal Stem Cells (hMSCs) labelling in FBS added medium.^[19] Indeed, the investigation of the interaction between these cells and nanoparticles is rising a significant attention, because, on one hand, of the possible application, ranging from drug delivery^[20] to magnetic resonance imaging,^[21] and, on the other hand, of the various aspects involved in such interactions,^[22] which can exhibit a significant dependence on the cell type.^[23] On this basis, by considering the possible enhancement of silica NP in hMSCs uptake due to FBS-free incubation and in order to contribute to the elucidation of the corona formation/influence, in this work we carried out a systematic investigation of the effect of difference in FBS concentration, stepwise ranging from 0 to 10% v/v, used to complement Dulbecco-Modified Eagle's Medium (hereafter DMEM), in the internalization of IRIS Dots by hMSCs. In particular, attention was paid to carry out physical chemical investigation of NP suspended in incubation media in conditions corresponding as much as possible to those experienced by nanoparticles when actually administered to cell cultures, in order to attain quantitative determinations of the NP dispersion and coverage of NP surface by adsorbed proteins actually "seen" by cells. As for the latter point, amounts of irreversibly adsorbed proteins (the so called "hard corona") were determined by thermogravimetry, augmented by spectroscopic measurements of the reversible fraction. Moreover, ζ -potential and CD-UV measurements were carried out to obtain complementary insights on the surface coverage by hard corona proteins.

2. Results and Discussion

2.1. FBS adsorption on IRIS Dots

2.1.1. Agglomeration vs dispersion of IRIS Dots in the incubation media

The state of IRIS Dots suspended in water, in DMEM and then added in such form to DMEM with different FBS concentration (1.0, 2.5, 6.0, 10.0% v/v) was investigated in terms of hydrodynamic radius (R_H) and ζ -potential (**Figure 1**; raw DLS data in **Figure S1** in the Supporting Information, hereafter SI). R_H was measured both keeping not adsorbed proteins in the suspension media (curve a) and removing them, i.e. leaving NP covered by the protein hard corona suspended in bare DMEM (curve a'). This latter condition was also used for the measurements of ζ -potential (curve b). Nanoparticles resulting from the synthesis and suspended in distilled water (pH 5.5) exhibited a R_H of ca. 25 nm (full circle), in good agreement with the mean size observed by TEM (d_m 50 nm \pm 2 nm),^[17] indicating they are basically monodispersed.

(part of the page left intentionally blank, in order to display together

Figure 1 and related caption in the next page)

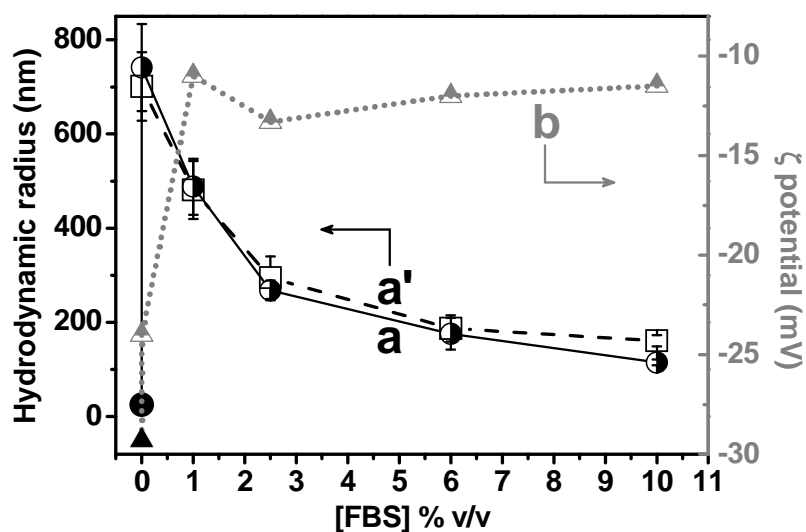


Figure 1. Results of the measurements of hydrodynamic radii (curves a,a'; data from mass distribution, Y values on the left axis) and ζ potential (curve b, Y values on the right axis) of: IRIS Dots suspended in distilled water (full symbols), DMEM and: a) DMEM with increasing FBS concentrations (for hydrodynamic radii); a', b) resuspended in DMEM after incubation in DMEM with increasing FBS concentrations, centrifugation/washing cycles. The distribution of R_H for each sample was monomodal, as indicated by the similarity of the values resulting from mass and number distributions; see Figure S1 in the SI. All data were collected after 1 h of suspension on the relevant suspending medium. The dispersion state of NP suspended for 6 h in bare DMEM and DMEM complemented with 1% v/v and 10% v/v FBS, and no significant changes with respect incubation time of 1 h were observed (Figure S1 in the SI).

Conversely, the suspension of IRIS Dots in bare DMEM resulted in a significant increase of R_H to ca. 740 nm, indicating the occurrence of particle agglomeration. Then, aliquots of NP suspended in DMEM were added to aliquots of culture medium containing different amount of FBS, ranging from 1.0 to 10.0% v/v (with respect the final volume of 5 mL) and incubated for 1h. DLS measurements revealed that, independently on the presence/absence of protein left in the incubation media, larger the amount of FBS used for the incubation, smaller the hydrodynamic radius of the agglomerates, which decreased down to ca. 120/160 nm for NP contacted with 10.0% v/v FBS (Figure 1, curve a, a'). When present, FBS proteins in solution exhibited a R_H of ca. 4 nm, in agreement with literature data.^[13 in SI] The observed

trend clearly indicates that adsorbed FBS proteins forming the corona acted as dispersing agents. However, the formation of a protein layer ca. 90/110 nm thick on hypothetically monodispersed nanoparticles in the case of 10.0% v/v FBS in DMEM (total R_H ca. 120/140 nm; radius of single nanoparticles ca. 25 nm) appeared unrealistic with respect to literature data dealing with the thickness of protein corona reported in the literature even for higher FBS concentration.^[3]

It can be concluded that a complete redispersion of IRIS Dots was not attained in the FBS concentration range considered in this investigation.

The inverse dependence of NP dispersion on the FBS concentration indicated that the process should be mainly driven by diffusion (typically dependent on concentration gradients) of proteins within preformed NP agglomerates. Hence, by considering that the distribution of R_H values remained monomodal (see Figure S1 in the SI), it can be proposed that serum proteins can diffuse from the medium throughout the inter-particle spaces in the agglomerates and, by reaching, for equivalent time of diffusion, inner layers in dependence on the FBS concentration, trigger a process of partial redispersion. This resulted in a disruption from larger to smaller agglomerates, stable and resistant to further protein diffusion for the given FBS concentration (if not, a further NP dispersion should occur). Thus, systems obtained by adding aliquots of the initial suspension of NP in DMEM to culture media with different FBS concentrations can be depicted as a series of suspensions of progressively smaller agglomerates with proteins mainly adsorbed on their surface. This scenario is reinforced by the trend exhibited by the ζ potential (Figure 1, b), which: i) slightly increased from ca. -29.3 to ca. -24.0 mV passing from monodispersed NP in pure water to the largest agglomerates in bare DMEM, ii) increased to ca. -11.5 mV for agglomerates separated from the 1.0% v/v FBS incubation medium, and iii) remained almost constant for agglomerates separated from incubation media containing higher amount of serum. By considering that ζ potential of FBS solution in DMEM was of ca. -9.4 mV, this trend agree with the presence in all IRIS

Dots/FBS DMEM systems of agglomerates almost completely covered by a hard corona, masking possible contribution to ζ potential from the surface of silica nanoparticles.

2.1.2. Quantitative study of FBS adsorption on IRIS Dots

As a next step, amount of adsorbed proteins and related surface coverage were determined. This latter is typically calculated by taking into consideration specific surface (SSA, $\text{m}^2 \cdot \text{g}^{-1}$) of the adsorbing solid. However, it must be considered that SSA of IRIS Dots was measured by adsorbing N_2 molecules on agglomerated NP (they were in a dry state, see Experimental Section), but gaseous nitrogen diffuse effectively within inter-nanoparticles voids, obviously providing a value corresponding to the contribution to the surface extension of all NP present in a unit mass of the material. Conversely, the data presented in the previous section indicated that the suspension of IRIS Dots in FBS-DMEM solutions should be constituted by NP agglomerates, which resisted the inner diffusion of proteins, the adsorption of which likely remained limited to the external surface of NP agglomerates. To this aim, the amount of proteins adsorbed by IRIS Dots in equilibrium with culture media containing different concentration of FBS was reported both per mass unit of NP and per unit of the external surface of agglomerates (**Figure 2**, section A and B, respectively). Such surface was calculated by assuming a simple spherical model of agglomerates, with radius equal to the measured R_H . This resulted in an overestimation of their actual size, because also the protein corona and the hydration shell contributed to the hydrodynamic radius. As for the evaluation of the silica mass present in an agglomerate, basic points were the volume and the density, and then the mass, of each NP.^[17] The inner volume of a spherical agglomerate of radius R_H actually occupied by IRIS Dots was estimated by multiplying the total volume for the occupancy factor for solids resulting from an hexagonal packing of identical spheres, as observed for these NP.^[17] The occupied volume was then divided by the volume of each NP,

obtaining an estimation of the number of IRIS Dots, and then of their overall mass, present in an agglomerate. The input values and the results of this procedure are summarized in **Table 1**.

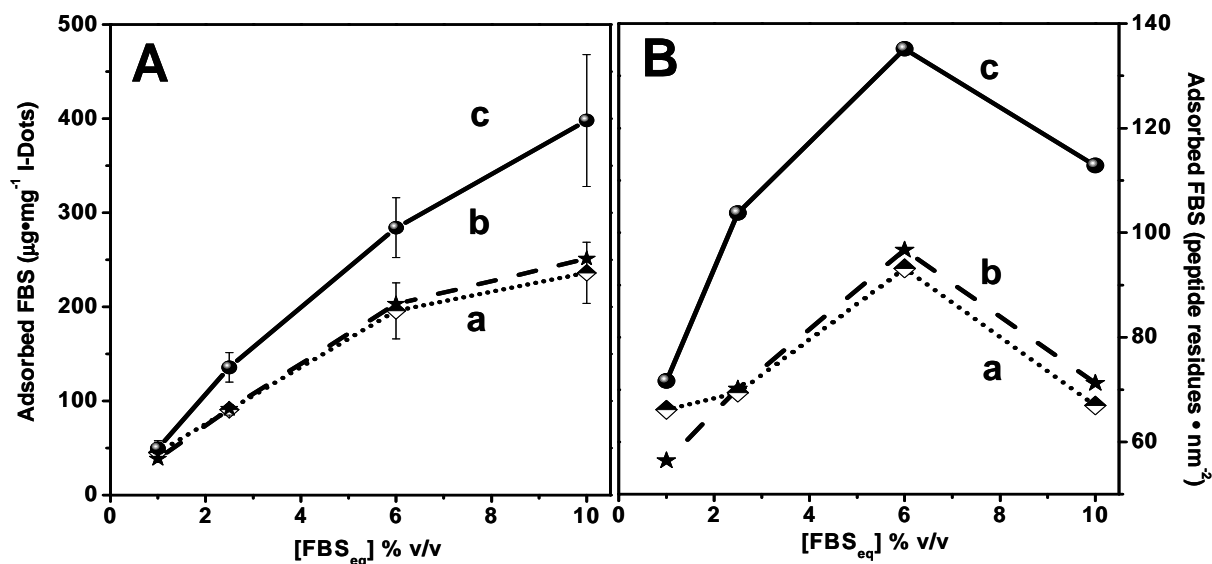


Figure 2. Adsorption isotherms of FBS on IRIS Dots: (a) amounts of irreversibly adsorbed proteins, i.e. protein hard corona, measured by TGA, (b) hard corona and (c) hard corona+reversibly adsorbed proteins measured by spectrophotometric analysis (Absorbance at $\lambda=280$ nm). The amounts are reported per mass unit (panel A) and estimated specific surface area of IRIS Dots agglomerates (panel B). Details in the text.

Table 1. Specific Surface Area of the IRIS Dots agglomerates available for protein adsorption at each FBS concentration.

FBS concentration [%v/v]	Hydrodynamic radius of agglomerates, Hr [nm]	IRIS Dots density ^{a)} [$\text{g}\cdot\text{cm}^{-3}$]	Hexagonal packing factor ^{b)}	Agglomerate density [$\text{g}\cdot\text{cm}^{-3}$]	Assumed Specific Surface Area for NP agglomerates, SSA_{agg} [$\text{m}^2\cdot\text{g}^{-1}$]
0	740				2.6
1.0	488				3.9
2.5	268	2.2	0.74	1.63	7.6
6.0	176				12.2
10.0	115				20.5

^{a)}form reference 17; ^{b)}from reference 24.

Focusing on the amount of adsorbed protein per NP mass unit, a monotonous increase by increasing the FBS equilibrium concentration was obtained (Figure 2A). Similar amounts of hard corona proteins were obtained from gravimetric measurements (Figure 2A, curve a),

insensitive to the actual composition of the adsorbed protein pool (expected to be different from the pool in solution), and from measurement of the absorbance intensity at 280 nm, due to aromatic residues in FBS proteins remained in the incubation media (Figure 2A, curve b). On the basis of such similarity, the amount of reversibly adsorbed proteins can be simply evaluated from the difference between the total amount of adsorbed proteins (determined only spectroscopically, Figure 2A, c) and the amount of proteins in the hard corona (Figure 2A, a, b). Hence, data indicated that for a 1.0% v/v FBS concentration, essentially only hard corona proteins were present of NP agglomerates, while higher FBS contents resulted in the occurrence also of a reversible adsorption, which finally accounted for almost 50% of the total amount of adsorbed proteins.

Turning to the estimation of the coverage of agglomerates by proteins, the complexity of FBS prevented the possibility to calculate theoretical amounts corresponding to a monolayer on the basis of the surface area occupied by one adsorbed protein, as typically carried out in the case of BSA absorption.^[25]

Thus, in the present case the surface coverage was evaluated in terms of number of peptide units per nm²: being known the average aminoacid composition of proteins (see **Table S2** of SI) and the weight of each kind of aminoacids, the mass amount of adsorbed proteins were easily converted in number of adsorbed peptide units. Once reported per surface unit of NP agglomerates and as a function of the FBS concentration in the incubation media, volcano curves were obtained (Figure 2B). At present it is rather difficult to propose an explanation for such a trend, likely resulting from the interplay among various factors, but a quite interesting insight is present in these data: even considering only hard corona proteins (Figure 2B, curves a and b), a minimum amount of ca. 55 peptide units per nm² was found. By considering that the surface area of IRIS Dots agglomerates was overestimated (see above), and the actual amount of protein adsorbed per surface unit area should be even higher, the

data reported above clearly indicate that NP agglomerates are completely covered by a protein corona, even at the lowest FBS concentration considered (1.0% v/v).

This scenario is in agreement with the trend exhibited by the ζ -potential (Figure 1, b, and related comments) which monitored the complete masking of the silica surface by adsorbed proteins.

2.2. Spectroscopic investigation of adsorbed proteins

Additional investigations aimed at complementary insights on the layers of adsorbed proteins were performed by CD-UV spectroscopy.

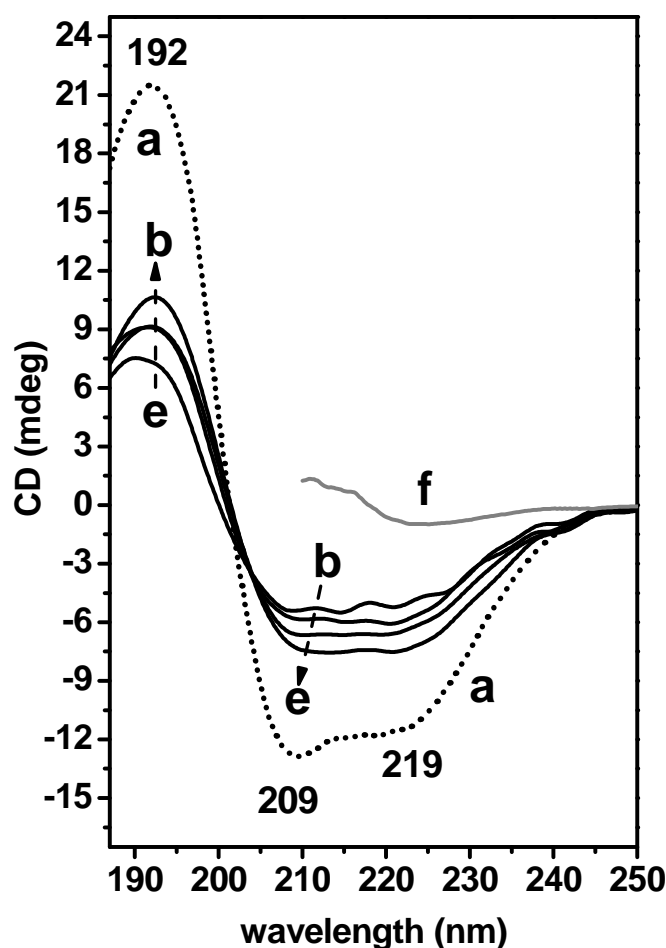


Figure 3. CD-UV spectra of FBS in solution (curve a, dotted line), denatured with GdHCl 6M (curve f, gray line) and irreversibly adsorbed on IRIS Dots after incubation in DMEM with 1.0, 2.5, 6.0 and 10.0% v/v FBS (curves b, c, d and e, respectively), centrifugation/washing cycles. After the last centrifugation, nanoparticles were suspended in distilled water, to attain a proper transparency in the spectral range investigated.

Figure 3 shows the CD-UV spectrum of FBS in DMEM (curve a), compared with the spectra of the hard protein corona resulting from the incubation of IRIS Dots in the culture media with different FBS concentrations (curves b-e). The comparison is extended to the spectrum of FBS in DMEM added with guanidine hydrochloride (GdHCl) 6M, in order to attain a complete denaturation of proteins (Figure 3, curve f, limited to 210 nm toward shorter wavelengths, because of the total absorption due to the denaturing agent). As reported in detail in the SI (Figure S2 and comment), the spectra were treated in order to compare their intensity on the basis of a similar content in proteins. The spectrum of FBS in the culture media (Figure 3, curve a) exhibits a profile constituted by a positive signal at 192 nm (left hand polarized $\pi \rightarrow \pi^*$ transition) and two negative components at 209 (right hand polarized $\pi \rightarrow \pi^*$ transition) and 219 nm ($n \rightarrow \pi^*$ transition), which should result from a prevalence of α -helix motifs in the structure of FBS proteins,^[26,27] in agreement with the typical composition of such protein pool.^[28] Conversely, no signals were observed in the transparency region of FBS solution treated with guanidine hydrochloride, as expected for a complete denaturation. Indeed, random coil proteins produce a negative CD signal below 210 nm. The spectra of proteins in the hard corona adsorbed on IRIS Dots (Figure 3, curves b-e) appeared significantly different in intensity and shape with respect to the case of FBS in solution (Figure 3, curve a), but still exhibited components at $\lambda \geq 210$ nm, indicating that a complete denaturation did not occur. In particular, the negative band at 222 nm due to α -helical motifs decreased in intensity in favor of a negative signal at longer wavelength. A similar spectral behavior was attributed to the formation of interprotein β -sheet structures by interaction among proteins with a prevalent α -helix structure,^[29] and, in the present case, well agrees with the formation of adsorbed protein multilayers proposed above. For the sake of completeness, it must be also considered that additional effects could have contributed to the observed

changes in the CD-UV spectral profiles, because the composition of the hard corona is expected to differ with respect to the initial protein pool in solution.^[30]

2.3. Check of IRIS Dots states in cellular environment

A qualitative check of the dispersion states of IRIS Dots in culture media during cell culture was then carried out, as link between cell-free and cellular experiments. In this respect, the external cellular microenvironment was analyzed by confocal microscopy and transmission electron microscopy (TEM). In summary, NP agglomerates were detected in great amount by confocal microscopy in the extracellular milieu for cells treated with serum-free IRIS Dots, they appeared barely detectable for cells incubated with 1.0% serum-added IRIS Dots and negligible in the other serum-added conditions (**Figure S3** in the SI). To confirm the observation that the aggregation state of nanoparticles decreases as the serum content increases, the number and the mean area of the NP aggregates was evaluated (Table S3 in the SI). TEM analysis (**Figure 4**) allowed high resolution imaging of NP and hMSCs interaction in different culture conditions, 0% (panels A-C), 1.0% (panels D-F) and 10.0% (panels G-I) v/v FBS, after 1h of incubation. In all samples NP could be observed both outside the cell membrane (panels A, D, G), near pseudopodia, and inside intracytoplasmic vesicles (panels B, C, E, F, H, I). In particular, Figure 4B illustrated NP aggregates in different phases: some completely outside of the cell (arrowheads), other located in deep invaginations of the cell membrane (arrow) and finally others embedded into intracytoplasmic vesicles (circles). Moreover, TEM analysis confirmed that the absence of serum in the culture medium results in a higher agglomeration of NP (panels A-C). At 1.0% (panels D-F) and 10.0% (panels G-I) v/v of FBS, NP agglomerates are smaller and more distant from each other. Quantitative analysis confirmed that NP in 0% FBS condition exhibited a significantly higher density ($\text{NP}\cdot\mu\text{m}^{-2}$, $p<0.01$) than in 1% and 10% FBS (bottom row of Figure 4).

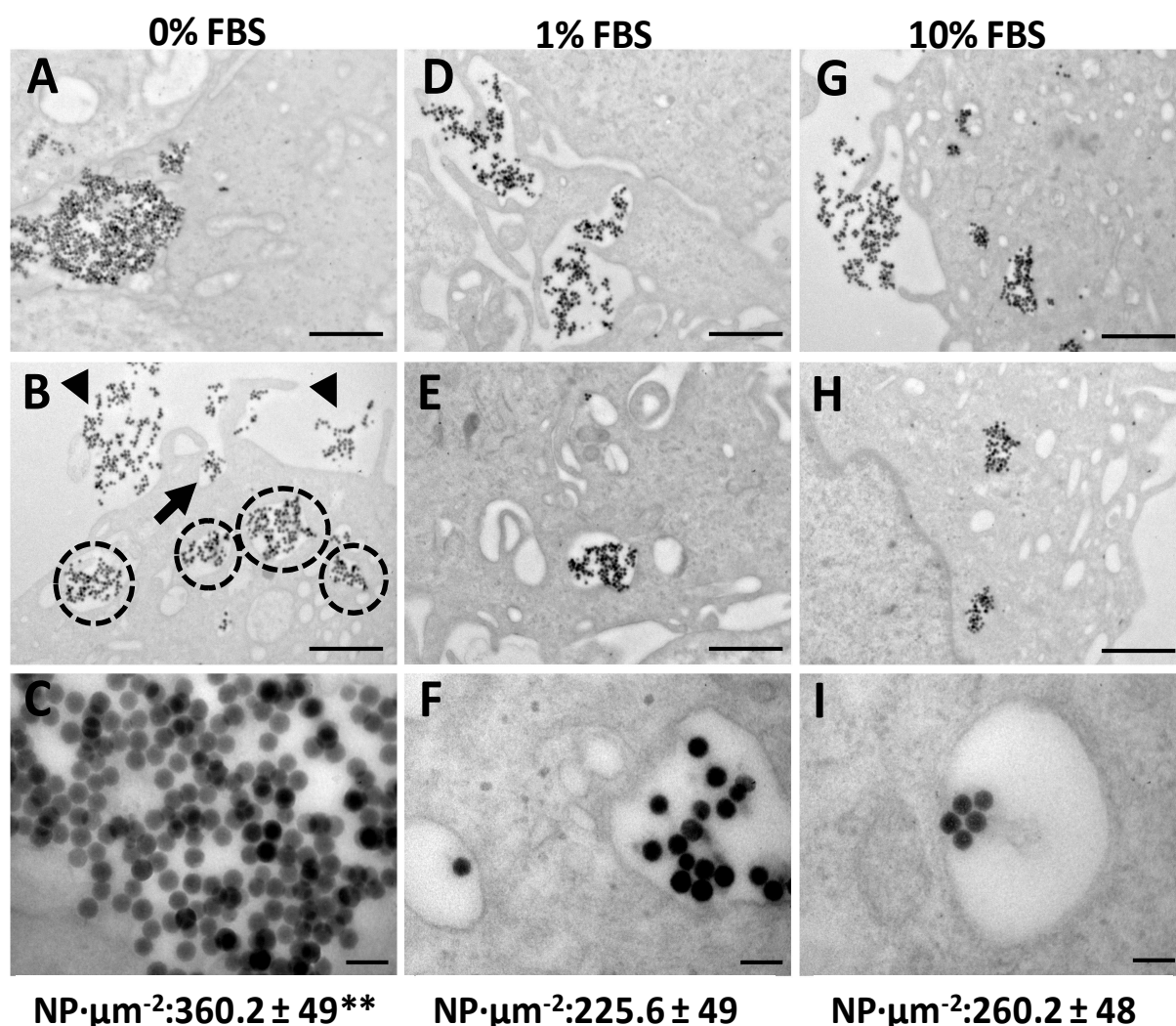


Figure 4. Transmission Electron Microscopy images of hMSCs after 1 h of incubation with $20 \mu\text{g}\cdot\text{mL}^{-1}$ IRIS Dots in serum free DMEM (A-C), and DMEM added with 1.0% (D-F) or 10.0% (G-I) v/v FBS. Scale bars: A, B, D, E, G, H: $1\mu\text{m}$; C, F, I: $0.1\mu\text{m}$. **Arrowheads**: NP aggregates completely outside of the cell. **Arrow**: NP aggregates located in deep invaginations of the cell membrane. **Circle**: NP aggregates embedded into intracytoplasmic vesicles. Mean \pm standard deviation of TEM measurements of the NP density in the three experimental groups (0%, 1%, 10% FBS) is reported (** $p\leq 0.01$). Images representative of data obtained by observing for from 3 to 5 sections, each containing 1000-2000 cells, for each sample (See Experimental section).

2.4. Quantitative study of IRIS Dots cellular uptake

To obtain a quantitative time course of IRIS Dots internalization in hMSCs incubated with different serum conditions, flow cytometry experiments were performed. IRIS Dots were pre-incubated for 1 h in the same DMEM based media used for cell free experiments (serum free; added with 1.0, 2.5, 6.0, 10.0% v/v FBS) and then administered at $20 \mu\text{g mL}^{-1}$ to plated hMSCs for increasing incubation times from 15 to 360 min. Before cell detachment and harvesting for flow cytometry analysis, all samples were extensively washed with PBS in order to remove excess IRIS Dots passively adsorbed on the cell surface.

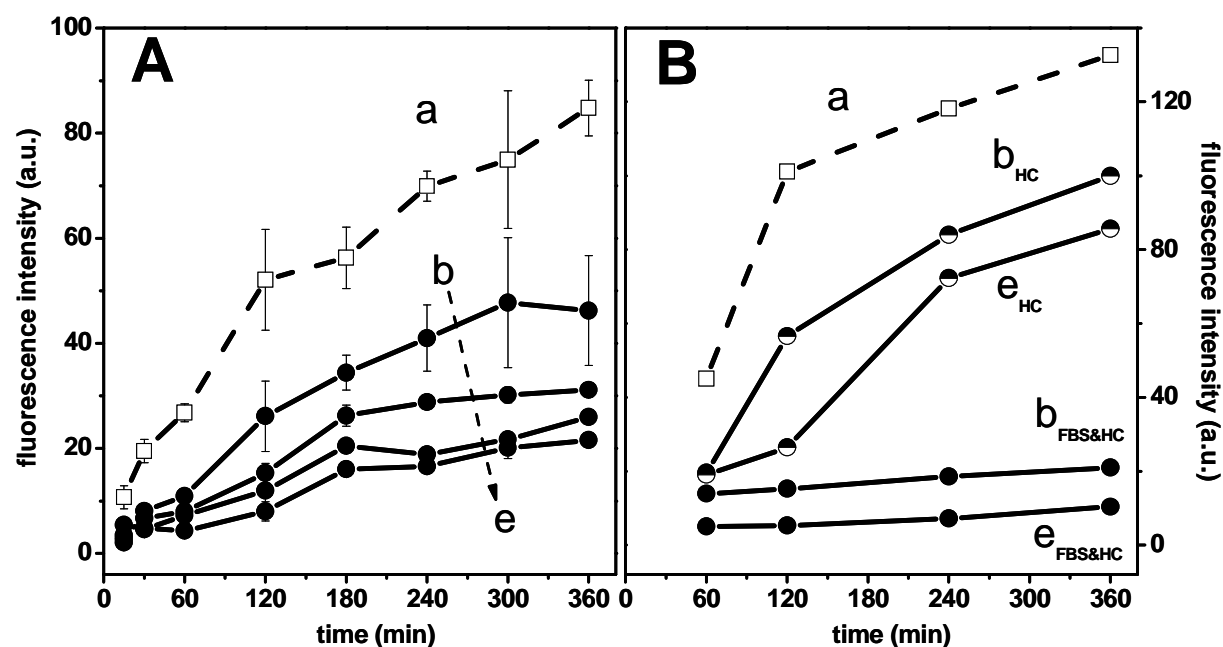


Figure 5. Kinetics of uptake of $20 \mu\text{g}\cdot\text{mL}^{-1}$ IRIS Dots by hMSCs as determined by flow cytometry. The mean fluorescence intensity of 10000 cells was determined for each replicate. Panel A: uptake in a) serum free DMEM (curve a) and b-e) DMEM added with 1.0, 2.5, 6.0 and 10.0 % v/v FBS, in the order). Error bars represent the standard error of the mean fluorescence intensity in 3 independent experiments. Panel B: a, b_{FBS&HC}, e_{FBS&HC}) uptake as in the conditions of the curves a, b, e in panel A; b_{HC} and e_{HC}) uptake in serum free DMEM of IRIS Dots carrying the protein hard corona resulting from the incubation in DMEM added with 1.0 and 10.0 % v/v FBS, respectively. The mean fluorescence intensity of 10000 cells was determined and one representative experiment of two is shown.

A monotonous increase of mean cell fluorescence intensity during the time course of hMSCs incubation was obtained in all cases (**Figure 5A**), indicating that NP internalization is a time-dependent process. Significant differences were observed in dependence on the composition of the incubation media: cells incubated with IRIS Dots in serum-free medium (Figure 5A, curve a) exhibited an uptake rate significantly higher compared to uptake rates observed for serum-added samples, which, in turn, decreased as the FBS content in the incubation medium increased (Figure 5A, curves b-e). It must be considered that the switch from “serum-free medium” to “serum-added medium” involved the simultaneous change in three experimental parameters: i) the extent of agglomeration of NP approaching cells (see Figures 1, 4 and S3 in the SI), ii) the presence/absence of a protein corona on NP agglomerates and iii) possible sensitivity of the uptake cell behavior to the presence/absence of serum in the culture medium. In order to elucidate, at least in part, the effectiveness of these parameters, the role of the hard corona in uptake cell behavior in the presence or absence of FBS was investigated. To this aim, IRIS Dots were pre-incubated in 1.0 and 10.0 % v/v FBS/DMEM, then one aliquot was kept in the pre-incubation medium, whereas another aliquot was carefully washed (see Experimental Section for details), filtered to isolate NP coated with protein hard corona and redispersed in serum-free medium. Hence, for each FBS concentration two sets of nanoparticles were obtained, one carrying the protein hard corona on the surface of NP agglomerates and kept in FBS added medium (condition hereafter referred to as FBS&HC) and the other only carrying the protein hard corona (condition hereafter referred to as HC). The samples were analyzed by DLS, and the results indicated that the presence /absence of FBS in the suspending medium did not affect significantly the size of NP agglomerates, as the R_H values obtained were 481/488 nm and 160/115 nm for incubation media containing 1.0 and 10.0 % v/v FBS, respectively (Figure S1 and Table S1 in the SI). These results appeared in agreement with data in Figure 1, dealing with NP coated with the protein hard corona, separated by the incubation medium by centrifugation and resuspended in serum-free medium.

The four sets of NP were administered to hMSCs following the same protocol reported above and the internalization was monitored by flow cytometry. For the sake of completeness, a control sample was included administering NP pre-incubated in bare DMEM (resulting in IRIS Dots agglomerates with R_H of ca. 740 nm, see Table 1) to cells kept in serum free conditions. As for the previous set of measurements reported in Figure 5A, a significantly faster increase of mean cell fluorescence intensity was obtained for the control (**Figure 5**, panel B, curve a) with respect to cells contacted with IRIS Dots pre-incubated and administered in FBS added conditions (Figure 5B, curves $b_{\text{FBS\&HC}}$, $e_{\text{FBS\&HC}}$). Conversely, cells contacted in FBS free condition with IRIS Dots carrying the protein hard corona exhibited an increase in mean fluorescence intensity significantly closer to the control (Figure 5B, curves b_{HC} , e_{HC}). By considering that the size of IRIS Dots agglomerates was the same within each pair of experiments reported in curves $b_{\text{FBS\&HC}}/b_{\text{HC}}$ and $e_{\text{FBS\&HC}}/e_{\text{HC}}$, the difference in uptake rate between FBS&HC and HC conditions appeared to depend only on the presence/absence of serum in the incubation medium. This behavior appeared different with respect to the results reported by Lesniak et al.,^[7, 30] but in such case lung epithelial cells were used, and silica NP remained almost monodispersed when administered.

To evaluate the possibility that the different uptake level was due to the different cellular metabolism in different serum conditions, another set of experiments was performed using CellTiterBlue assay. hMSCs were treated with both IRIS Dots and CellTiterBlue in serum free and serum added (1.0 and 10.0 % FBS v/v) conditions and the level of mitochondrial metabolism was analyzed through the resulting mean fluorescence intensity. As shown in **Figure 6** panel A, the 10% serum added condition significantly reduced the cellular metabolism, while serum free and 1% serum added conditions did not show statistically significant differences. This observation could partially explain the decrease of uptake rate as the content of serum in incubation medium increased observed in Figure 5A curves b-e.

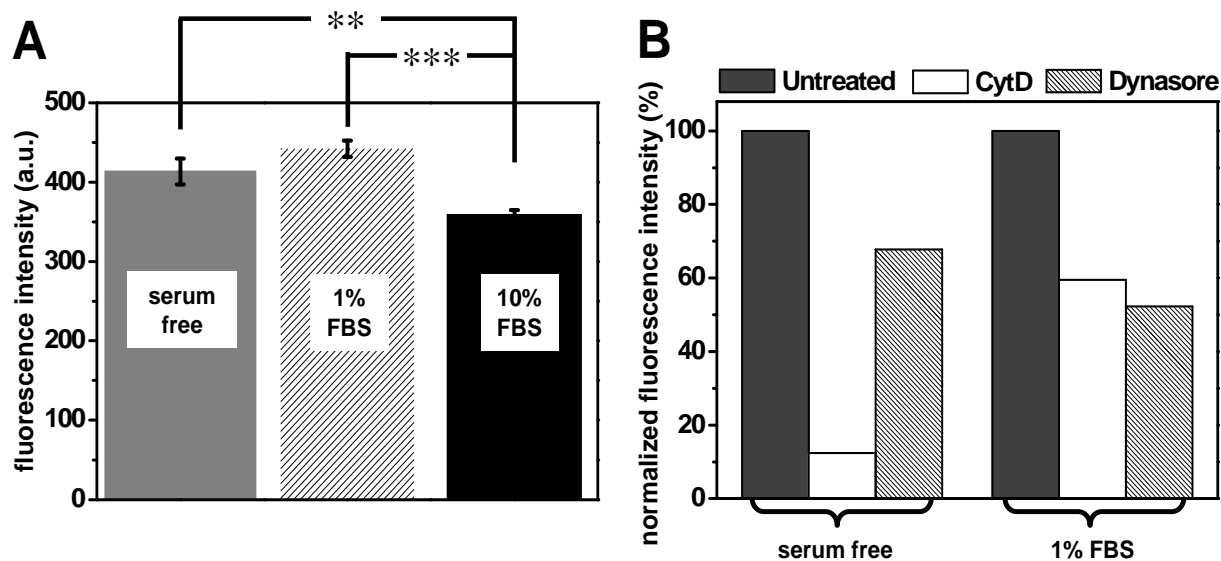


Figure 6. A) Mean fluorescence intensity of the medium of hMCSs incubated both with IRIS Dots $20 \mu\text{g}\cdot\text{mL}^{-1}$ and CellTiter Blue in absence and presence 1% and 10% v/v of FBS in DMEM. (** $p < 0.01$; *** $p < 0.001$). B) IRIS Dots uptake level as determined through flow cytometry after treatment with Cytochalasin D and Dynasore in absence and presence of 1% of FBS in DMEM. The values were expressed as the percentage of mean fluorescence intensity of 10000 treated cells respect on the mean fluorescence intensity of 10000 untreated cells.

The possibility that different mechanisms of internalization could be the explanation for the different uptake level between serum free and 1.0% serum added conditions was then evaluated. To this purpose, the NP uptake was tested in the presence of two different pharmacological inhibitors: Cytochalasin D (CytD), which inhibits actin-related phagocytosis and non-clathrin-non-caveole-dependent endocytosis, and Dynasore, which inhibits the clathrin-caveole dependent endocytosis. Because of the ability of the cells to elude one inhibiting pathway through the redundant activation of other mechanisms normally not involved, a short incubation time was chosen for treating cells with IRIS Dots and inhibitors. Figure 6 B shows that the presence of inhibitors decreases the NP uptake level for both serum free and 1% serum added conditions. However, it is interesting to underline that in serum free condition the uptake seems to be mainly dependent on actin-related phagocytosis and non-clathrin-non-caveole-dependet endocytosis, while in the 1% serum added condition the main mechanism involved was the clathrin-caveole dependent endocytosis.

Altogether, these results suggest that the presence and amount of serum proteins is crucial for determining the NP uptake level of hMSCs, because it influences both the cellular metabolism and the endocytic pathway involved.

3. Conclusion

The collection of results obtained in this work allows to propose some conclusions dealing with methodological aspects, insights on silica nanoparticles-serum interaction and the role of free and adsorbed proteins in the uptake of nanoparticles by hMSCs.

As for the first aspect, the combination of thermogravimetry and spectroscopy seem to be effective in determining both the irreversible and reversible amounts of adsorbed serum proteins. Moreover, the attainment of complete surface coverage of nanoparticles by the protein hard corona can be monitored by combining ζ -potential and CD-UV measurements. When silica nanoparticles agglomerate in culture media, the surface of the agglomerates can be completely covered by a hard corona even for serum proteins concentration as small as 1.0% v/v. At higher concentration proteins act as dispersing agents, but, because of the higher amount of proteins in the incubation media, the external surface of the smaller agglomerates can still be covered by a complete hard corona. Consequently, cells can always “see” the surface of protein layers adsorbed on nanoparticles even changing the serum content in the 1.0-10.0% v/v range. The uptake of silica nanoparticles by hMSCs appears more sensitive to the absence/presence of serum proteins in the culture media than to the absence/presence of the adsorbed protein corona or the size of agglomerates. As for this latter, a direct relationship with respect to the uptake rate seems to be effective. *In vitro* experiments to evaluate the cellular uptake kinetics, cellular metabolism and involved endocytic pathway showed a great impact of the presence/absence of serum in these parameters. Our results underline the importance of the study of different incubation condition in the experiments to obtain a more complete NP/cells scenario.

4. Experimental Section

Materials: N-hydroxysuccinimide (NHS) ester of IRIS3 cyanine was purchased from Cyanine Technologies srl (now Pianeta S.p.A.). Reagents and solvents used for preparation of IRIS Dots (tetraethylorthosilicate, aminopropyltriethoxysilane, cyclohexane, n-hexanol, Triton X-100, dimethylformamide and diethylether) as well as PBS (phosphate buffer saline), deuterated water and guanidine hydrochloride were high-purity Sigma-Aldrich products and used as received.

For both cell-free experiments and cell cultures Dulbecco-modified Eagle's Medium (DMEM) supplemented with 1% nonessential amino acids, kanamycin ($50 \mu\text{g}\cdot\text{mL}^{-1}$), 0.1% β -mercaptoethanol, all purchased from Gibco[®]Invitrogen, were used. Fetal bovine serum (FBS) was purchased from Gibco[®]Invitrogen,

Synthesis of IRIS3-Silane derivative and hybrid IRIS Dots: Cyanine-aminopropyltriethoxysilane derivative was prepared by adding aminopropyltriethoxysilane (APTS, 46.0 mol, 10 μL) to a cyanine NHS-ester solution in dimethylformamide (11.5 mol in 500 μL of DMF) and stirring for 24 hours at room temperature. The reaction was monitored by thin-layer chromatography (TLC) and mass spectrometry (MS) for the complete conversion of the NHS-esters in cyanine-APTS. The final products were separated from the unreacted APTS by dilution in diethylether and subsequent filtration to obtain powders as products. Hybrid IRIS3/silica nanoparticles (referred to as IRIS Dots) were prepared by using the reverse microemulsion method following the procedure reported in refs.17, 18, resulting in $5 \text{ mg}\cdot\text{mL}^{-1}$ suspension of IRIS Dots in distilled water.

Adsorption of serum proteins on nanoparticles: A “parent” suspension of IRIS Dots in bare DMEM was prepared as follows: four aliquots of 5 mL of the suspension of NP in water were centrifuged (10.000 rpm for 20 min), the supernatants removed and the resulting pellets resuspended in 2.5 mL of bare DMEM. Aliquots of 2.5 mL DMEM complemented with different amounts of FBS were then prepared and each of them added to one of the 2.5 mL suspensions of IRIS Dots in bare DMEM. The nominal concentrations of FBS in the four final volumes were 1.0, 2.5, 6.0 and 10.0% v/v. The samples, placed in centrifuge tubes were rotated end over end for 1h at 298 K. Separated experiments indicated that longer incubation times (2, 6, 12 h) did not result in a significant increase of the amount of adsorbed proteins. Samples were centrifuged at 10.000 rpm for 20 minutes at 298 K. The supernatants were then removed and IRIS Dots with adsorbed proteins underwent several re-suspension/centrifugation cycles in order to desorb reversibly adsorbed proteins. As re-suspending media, DMEM was used for the samples prepared for thermogravimetric analyses, while a buffered solution (0.01M phosphate buffer: pH 7.4, 0.138 M NaCl, 0.0027 M KCl), modified by addition of CaCl₂ and MgCl₂ to attain a content in Ca²⁺ and Mg²⁺ ions similar to that found in culture medium DMEM (8 mM and 200 μM, respectively) was used for the preparation of samples analyzed by spectrophotometry (*vide infra*).

Quantification of adsorbed proteins: The amount of FBS proteins adsorbed on IRIS Dots was determined by two complementary methods, thermogravimetry and spectrophotometry. Results of both series of measurements are reported as the mean value of at least three separate experiments ± standard error. As for the irreversibly adsorbed fraction, the so called “protein hard corona”, thermogravimetric (TGA) measurements were carried out (TA Instruments SDT Q600) on the FBS/IRIS Dots samples resulting from re-suspension/centrifugation cycles carried out using DMEM as washing medium. Samples were dried at room temperature in a vacuum oven, then 10 mg aliquots were placed in the sample

holder and the TGA measurements were performed under a constant air flux ($0.1 \text{ L}\cdot\text{min}^{-1}$), with a heating rate of $283 \text{ K}\cdot\text{min}^{-1}$, from room temperature to 1273 K.

For the sake of comparison, adsorption isotherms of serum proteins on IRIS Dots were also obtained by measuring spectrophotometrically the difference in protein concentration before and after contact with the powder. The specific aim was to obtain information also on the amount of reversibly adsorbed proteins. The usual method of determination of the amount of proteins in an aqueous solution by the spectroscopic measurement of the absorbance value at $\lambda = 280 \text{ nm}$ (hereafter A_{280}) was used. Because of the interference of some DMEM components (i.e. aminoacids) in the spectrophotometric detection of proteins, for these measurements serum was dissolved in the buffered solution indicated at the end of the previous section. The measure of the amounts of total (reversibly + irreversibly adsorbed) and irreversibly adsorbed proteins was carried out as follows:

i) a calibration curve A_{280} vs FBS concentrations (% v/v) was established (see **Figure S4** in the SI), including the A_{280} values corresponding to the initial FBS concentration in the incubation solutions (1.0, 2.5, 6.0, 10.0% v/v), hereafter $A_{280}(\text{initial})$

ii) after incubation, suspensions of IRIS Dots in FBS/buffer media were centrifuged (10.000 rpm per 20 min) and supernatants analyzed spectrophotometrically (Cary 300 Bio, Varian), in order to determine the Absorbance of proteins remained in solution, hereafter $A_{280}(\text{remained})$.

iii) the amount of adsorbed proteins was then derived on the basis of the following difference:

$$A_{280}(\text{initial}) - A_{280}(\text{remained}) \rightarrow \text{amount of total (reversibly + irreversibly) adsorbed proteins}$$

iv) the pellets of NP with adsorbed FBS resulting from the centrifugation underwent 3 re-suspension/centrifugation cycles using each time 5 mL of buffer as washing medium. For each sample, the 3 supernatants were merged and A_{280} measured, in order to determine the amount of reversibly adsorbed proteins, hereafter $A_{280}(\text{reversible})$.

v) finally, the amount of irreversibly adsorbed proteins was determined on the basis of the following difference:

$$[A_{280}(\text{initial}) - A_{280}(\text{remained})] - A_{280}(\text{reversible}) \rightarrow \text{amount of irreversibly adsorbed proteins}$$

Circular Dichroism UV spectroscopy (CD-UV): this spectroscopic method was used to evaluate changes in the secondary structure of irreversible adsorbed proteins. Solutions of 0.1 mg mL⁻¹ FBS, as received and denatured with 6M guanidine hydrochloride, were scanned in the far-UV spectral range (four accumulations) over the wavelength region 180-300 nm with a scanning speed of 50 nm min⁻¹ using a Jasco J-815 spectropolarimeter equipped with a Xe arc lamp, using a quartz circular cuvette (path length 0.1 mm). The analyses of the protein hard corona were performed on IRIS Dots incubated in FBS/DMEM solutions with different serum concentrations (see above), washed with DMEM (suspension/centrifugation cycles) and finally re-suspended in distilled water just before data acquisition (DMEM is non transparent in the spectral range of interest for these measurements).

Dynamic Light Scattering (DLS): DLS measurements were performed in a 90Plus Particle Size Analyzer (Brookhaven Instruments) at a laser wavelength of 660 nm and a detection angle of 90° at 20° C. Samples were prepared by suspending IRIS Dots in distilled water (pH 5.5), bare DMEM and DMEM complemented with 1.0, 2.5, 6.0 and 10.0% v/v FBS. In all cases the IRIS Dots concentration just before measurements was 20 µg·mL⁻¹. DLS plots are reported both as number weight and mass weight (Figure S1). Measurements were performed in triplicates.

ζ Potential: Surface potential of both bare IRIS Dots (suspended in distilled water and in DMEM) and IRIS Dots with hard corona proteins (suspended in DMEM) was evaluated by

electrophoretic light scattering (ELS) using a Zetasizer Nano-ZS, Malvern Instruments (Worcestershire, U.K.). IRIS Dots with the protein hard corona were obtained by the FBS adsorption procedure reported above, with final washing in DMEM.

Cell culture and IRIS Dots treatment: hMSCs isolated from the bone marrow of normal donors were purchased from Lonza Walkersville Inc. (Maryland, USA) and cultured in standard growth medium consisting of DMEM supplemented with 10.0% heat inactivated fetal bovine serum; cells were kept in an atmosphere of 5% CO₂ and 95% air at 310 K in a humidified incubator.

IRIS Dots 1 mg·mL⁻¹ were incubated in DMEM either alone or with 1.0-2.5-6.0-10.0% v/v FBS for 1 h. Pre-incubated IRIS Dots were used immediately or, in order to form and isolate HC-IRIS Dots, were subjected to several cycles of washing, recovered by filtration with Millipore nylon syringe filters (pore diameter of 50 nm) and re-suspended in DMEM. Because the laboratory in charge of cell tests was not equipped for centrifugation in sterile conditions, IRIS Dots coated with hard corona were separated from the incubation media by syringe filtration under sterile hood.

The procedure was as follows:

- i) IRIS Dots incubated with different FBS concentration in DMEM were filtered and washed by passing through the filter 1 mL of DMEM for 3 times;
- ii) filters with IRIS Dots carrying the hard corona (HC-IRIS Dots) were removed from the syringes and placed in falcons (15 mL), 5 mL of DMEM was added to each of them, and falcons were rotated end over end for 15 min;
- iii) filters were recovered and analyzed with a spectrophotometer (Horiba Jobin-Yvon Fluorolog 3; spectra collected in the “front face” mode for solid samples); in no case the photoemission typical of IRIS Dots ($\lambda_{\text{ex}} = 520 \text{ nm}$; $\lambda_{\text{em}} = 570 \text{ nm}$) was detected, indicating the removal of nanoparticles from the filters;

iv) each suspension of IRIS Dots removed from the filters was divided in two aliquots, one used for DLS measurements and quantification and the other for cell tests.

v) on the basis of the quantification, HC-IRIS Dots were prepared at a nominal concentration of $20 \mu\text{g}\cdot\text{mL}^{-1}$ and used for cell tests.

Detection of IRIS Dots uptake by hMSCs: To detect the uptake of IRIS Dots, hMSCs were seeded at $7000 \text{ cells cm}^{-2}$ in sterile eight-well μ -slides (Ibidi GmbH) or 25 cm^2 flasks or 6 well-plates respectively for confocal microscopy, transmission electron microscopy (TEM) and flow cytometry. After 24 h of culture in standard growth medium to allow cell attachment, cells were washed three times to remove serum and then treated with IRIS Dots as previously described.

For uptake analysis by confocal microscopy, green 5-Chloromethylfluorescein Diacetate (CMFDA) $5 \mu\text{M}$ was added for 30 minute before NP incubation. Fluorescence images of cells during NP incubation were obtained with a 510 Carl Zeiss confocal laser microscope using a 63x objective. The number and the mean area of the NP aggregates was analyzed with the ImageJ Plug-in “Analyze Particles” (<http://imagej.nih.gov/ij/>). For both TEM and flow cytometry analyses, cell were incubated with IRIS Dots $20 \mu\text{g}\cdot\text{mL}^{-1}$ and then washed extensively with PBS and harvested by trypsinization. For pharmacological inhibition, before trypsinization hMSCs were pre-treated for 30 minutes with Cytochalasin D ($1 \mu\text{M}$) or Dynasore ($80 \mu\text{M}$) in complete medium and then incubated with both IRIS Dots $20 \mu\text{g mL}^{-1}$ and inhibitors in serum free or 1% FBS v/v for 1 h. Untreated cells were used as control of the maximum uptake level.

For TEM analysis, the cell pellets were processed according to the procedure described by Raimondo et al.^[31] In brief, the pellets were fixed in 1% paraformaldehyde, 1.25% glutaraldehyde and 0.5% saccharose in Sørensen phosphate buffer (0.1 M, pH 7.2) for 2 h. After washing in 1.5% saccharose in Sørensen phosphate buffer (0.1 M, pH 7.2) for 6-12 h,

the pellets were post-fixed in 2% osmium tetroxide, dehydrated, and embedded in Glauert's embedding mixture^[32] consisting in equal parts of Araldite M and Araldite Harter, HY 964 (Merck, Darmstadt, Germany), containing 0.5% of the plasticizer dibutyl phthalate and 1–2% of the accelerator 964, DY 064 (Merck, Darmstadt, Germany). The specimens were cut using a Leica Ultracut UTCultramicrotome and the thin sections (70 nm) were examined in a JEM-1010 transmission electron microscope operating at 80 kW. For each experimental group from 3 to 5 sections (each of which can contain an approximate number of 1000- 2000 cells) were observed. The area of 50 aggregates, randomly selected in different cells, was measured and the relative number of NP counted. Results were then expressed in terms of density (NP·m⁻²). For flow cytometry analysis, the pellets were resuspended in PBS and fluorescence emission of IRIS Dots (FL-2) was analyzed on a CyAN ADP flow cytometer using the Summit 4.3 software (Beckman Coulter, Fullerton, California).

Metabolic assay: to evaluate different metabolic levels of cells, CellTiterBlue assay were used. In particular, the CellTiter-Blue contains resazurin which is reduced into the fluorescent resorufin by cellular reductases depending on the metabolic capacity of treated cells. hMSCs were seeded at 7000 cells cm⁻² in 24 well-plates and after 24 h of culture in standard growth medium to allow cell attachment, cells were washed three times to remove serum and then treated with IRIS Dots 20 µg mL⁻¹ and CellTiter Blue (1:20) in serum free and serum added (1.0 and 10.0% v/v). After 6 h of incubation, fluorescence of the medium was measured using Tecan Infinite® F200 microplate reader (Tecan Group Ltd, Switzerland). To exclude the influence of serum in the fluorescence intensity, the value of the blank without cells with the different serum conditions was subtracted to each sample. The mean of fluorescence intensity of three independent experiments were obtained for the various serum conditions. The statistical analysis was performed using t-test, ** p<0.01; *** p< 0.001.

Supporting Information

Supporting Information is available from the Wiley Online Library or from the author.

Acknowledgements

The research leading to these results received funding from Compagnia di San Paolo and University of Torino (project n. ORTO11RRT5) and from Mi.S.E.-ICE-CRUI (call 2010, registration number 0040898).

F.C. was the recipient of a PhD fellowship sponsored by the Compagnia di San Paolo.

- [1] D. Walczyk, F. B. Bombelli, M. P. Monopoli, I. Lynch, K. A. Dawson, *Journal of the American Chemical Society* **2010**, *132*, 5761-5768.
- [2] A. Lesniak, A. Campbell, M. P. Monopoli, I. Lynch, A. Salvati, K. A. Dawson, *Biomaterials* **2010**, *31*, 9511-9518.
- [3] M. P. Monopoli, D. Walczyk, A. Campbell, G. Elia, I. Lynch, F. B. Bombelli, K. A. Dawson, *Journal of the American Chemical Society* **2011**, *133*, 2525-2534.
- [4] Z. W. Lai, Y. Yan, F. Caruso, E. C. Nice, *Acs Nano* **2012**, *6*, 10438-10448.
- [5] M. P. Monopoli, C. Aberg, A. Salvati, K. A. Dawson, *Nature Nanotechnology* **2012**, *7*, 779-786.
- [6] S. Tenzer, D. Docter, J. Kuharev, A. Musyanovych, V. Fetz, R. Hecht, F. Schlenk, D. Fischer, K. Kiouptsi, C. Reinhardt, K. Landfester, H. Schild, M. Maskos, S. K. Knauer, R. H. Stauber, *Nature Nanotechnology* **2013**, *8*, 772-781.
- [7] A. Lesniak, A. Salvati, M. J. Santos-Martinez, M. W. Radomski, K. A. Dawson, C. Aberg, *Journal of the American Chemical Society* **2013**, *135*, 1438-1444.
- [8] D. Guarnieri, A. Guaccio, S. Fusco, P. A. Netti, *Journal of Nanoparticle Research* **2011**, *13*, 4295-4309.
- [9] L. C. J. Thomassen, V. Rabolli, K. Masschaele, G. Alberto, M. Tomatis, M. Ghiazza, F. Turci, E. Breynaert, G. Martra, C. E. A. Kirschhock, J. A. Martens, D. Lison, B. Fubini, *Chem. Res. Toxicol.* **2011**, *24*, 1869-1875.
- [10] J. N. Israelachvili, *Intermolecular and Surface Forces*, Academic Press, London, UK **1996**.
- [11] D. Drescher, G. Orts-Gil, G. Laube, K. Natta, R. W. Veh, W. Osterle, J. Kneipp, *Analytical and bioanalytical chemistry* **2011**, *400*, 1367-1373.
- [12] S. Kittler, C. Greulich, J. S. Gebauer, J. Diendorf, L. Treuel, L. Ruiz, J. M. Gonzalez-Calbet, M. Vallet-Regi, R. Zellner, M. Koller, M. Epple, *Journal of Material Chemistry* **2010**, *20*, 512-518.

- [13] G. Maiorano, S. Sabella, B. Sorce, V. Brunetti, M. A. Malvindi, R. Cingolani, P. P. Pompa, *ACS Nano* **2010**, *4*, 7481-7491.
- [14] L. Merhari, *Hybrid Nanocomposites for Nanotechnology*, Springer, New York, USA **2009**.
- [15] D. R. Larson, H. Ow, H. D. Vishwasrao, A. A. Heikal, U. Wiesner, W. W. Webb, *Chemistry of Materials* **2008**, *20*, 2677-2684.
- [16] S. Bonacchi, D. Genovese, R. Juris, M. Montalti, L. Prodi, E. Rampazzo, N. Zaccheroni, *Angewandte Chemie International Edition* **2012**, *50*, 4056-4066.
- [17] G. Alberto, I. Miletto, G. Viscardi, G. Caputo, L. Latterini, S. Coluccia, G. Martra, *Journal of Physical Chemistry C* **2009**, *113*, 21048-21053.
- [18] I. Miletto, A. Gilardino, P. Zamburlin, S. Dalmazzo, D. Lovisolo, G. Caputo, G. Viscardi, G. Martra, *Dyes and Pigments* **2010**, *84*, 121-127.
- [19] L. Accomasso, E. Cibrario Rocchietti, S. Raimondo, F. Catalano, G. Alberto, A. Giannitti, V. Minieri, V. Turinetto, L. Orlando, S. Saviozzi, G. Caputo, S. Geuna, G. Martra, C. Giachino, *Small* **2012**, *8*, 3192-3200.
- [20] B. Cao, M. Yang, Y. Zhu, X. Qu, C. Mao, *Advanced Materials* **2014**, *26*, 4627-4631
- [21] F. Tian, G. Chen, P. Yi, J. Zhang, A. Li, J. Zhang, L. Zheng, Z. Deng, Q. Shi, R. Peng, Q. Wang, *Biomaterials*, **2014**, *35*, 6412-6421.
- [22] I. V Ogneva, S. V Buravkov, A. N Shubenkov, L. B Buravkova, *Nanoscale Research Letters* **2014**, *9*, 284-294.
- [23] S. R. Saptarshi, A. Duschl, A. L Lopata, *Journal of Nanobiotechnology* **2013**, *11*: 26.
- [24] W. D. Callister, *Materials Science and Engineering: An Introduction*, Wiley, Versailles, KY, USA **2007**.
- [25] F. Turci, E. Ghibaudi, M. Colonna, B. Boscolo, I. Fenoglio, B. Fubini, *Langmuir* **2010**, *26*, 8336-8346.

- [26] S. M. Kelly, N. C. Price, *Biochimica Et Biophysica Acta-Protein Structure and Molecular Enzymology* **1997**, *1338*, 161-185.
- [27] S. M. Kelly, T. J. Jess, N. C. Price, *Biochimica Et Biophysica Acta-Proteins and Proteomics* **2005**, *1751*, 119-139.
- [28] S. Tenzer, D. Docter, S. Rosfa, A. Wlodarski, J. Kuharev, A. Reikik, S. K. Knauer, C. Bantz, T. Nawroth, C. Bier, J. Sirirattanapan, W. Mann, L. Treuel, R. Zellner, M. Maskos, H. Schild, R. H. Stauber, *Acs Nano* **2011**, *5*, 7155-7167.
- [29] D. M. Charbonneau, H.-A. Tajmir-Riahi, *Journal of Physical Chemistry B* **2009**, *114*, 1148-1155.
- [30] A. Lesniak, F. Fenaroli, M. R. Monopoli, C. Aberg, K. A. Dawson, A. Salvati, *Acs Nano* **2012**, *6*, 5845-5857.
- [31] S. Raimondo, C. Penna, P. Pagliaro, S. Geuna, *J. Anat.* **2006**, *208*, 3-12.
- [32] F. Di Scipio, S. Raimondo, P. Tos, S. Geuna, *Microscopy Research and Technique* **2008**, *71*, 497-502.

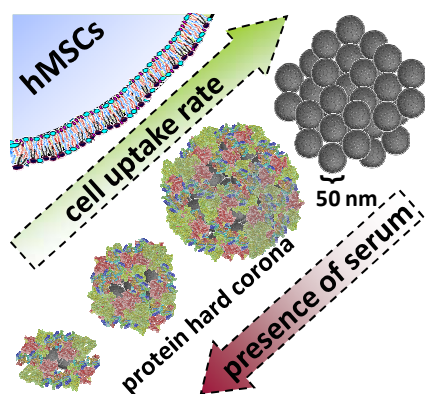
The absence of serum proteins in the culture media increases the uptake rate of dye-doped silica nanoparticles by mesenchymal stem cells. As a consequence, and because of the dispersing action of proteins, bare and large agglomerates of nanoparticles enter the cells more quickly than smaller agglomerates coated with a protein corona.

Keyword: Nanoparticles and mesenchymal stem cells

F. Catalano, L. Accomasso, G. Alberto, C. Gallina, S. Raimondo, S. Geuna, C. Giachino, G. Martra*

Title: Factors Ruling the Uptake of Silica Nanoparticles by Mesenchymal Stem Cells: Agglomeration vs Dispersions, Absence vs Presence of Serum Proteins

ToC figure



Supporting Information

Factors Ruling the Uptake of Silica Nanoparticles by Mesenchymal Stem Cells: Agglomeration vs Dispersions, Absence vs Presence of Serum Proteins

Federico Catalano, Lisa Accomasso, Gabriele Alberto, Clara Gallina, Stefania Raimondo, Stefano Geuna, Claudia Giachino and Gianmario Martra*

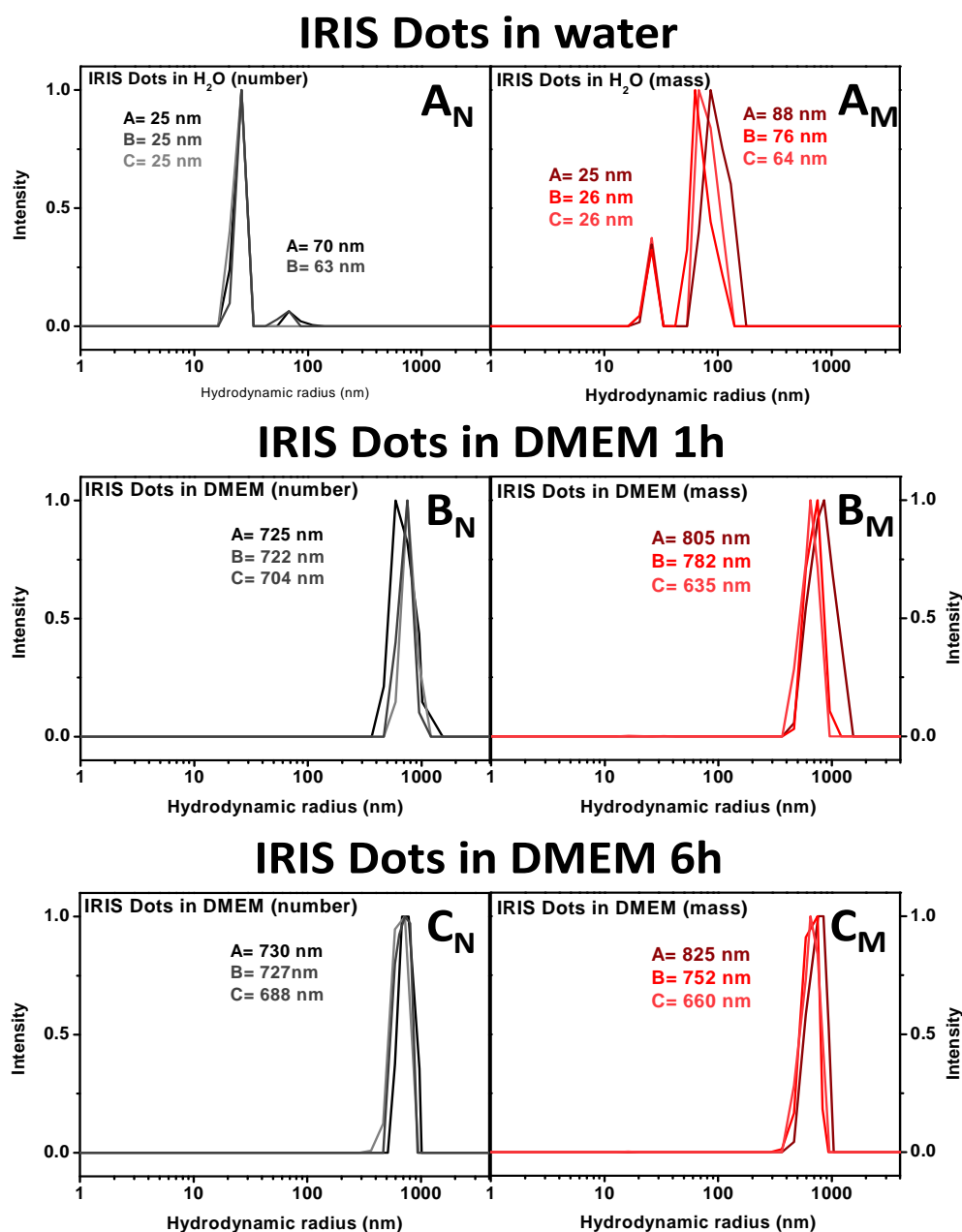


Figure S1. Raw data of DLS measurements related to R_H values presented in the main text. All the data are presented both in number (left panels, labeled as “X_N”) and mass (right panels, labeled as “X_M”) distributions. Each measure of the triplicates is reported: IRIS Dots in water (A), IRIS Dots suspended in DMEM for 1 and 6 hours (B and C, respectively).

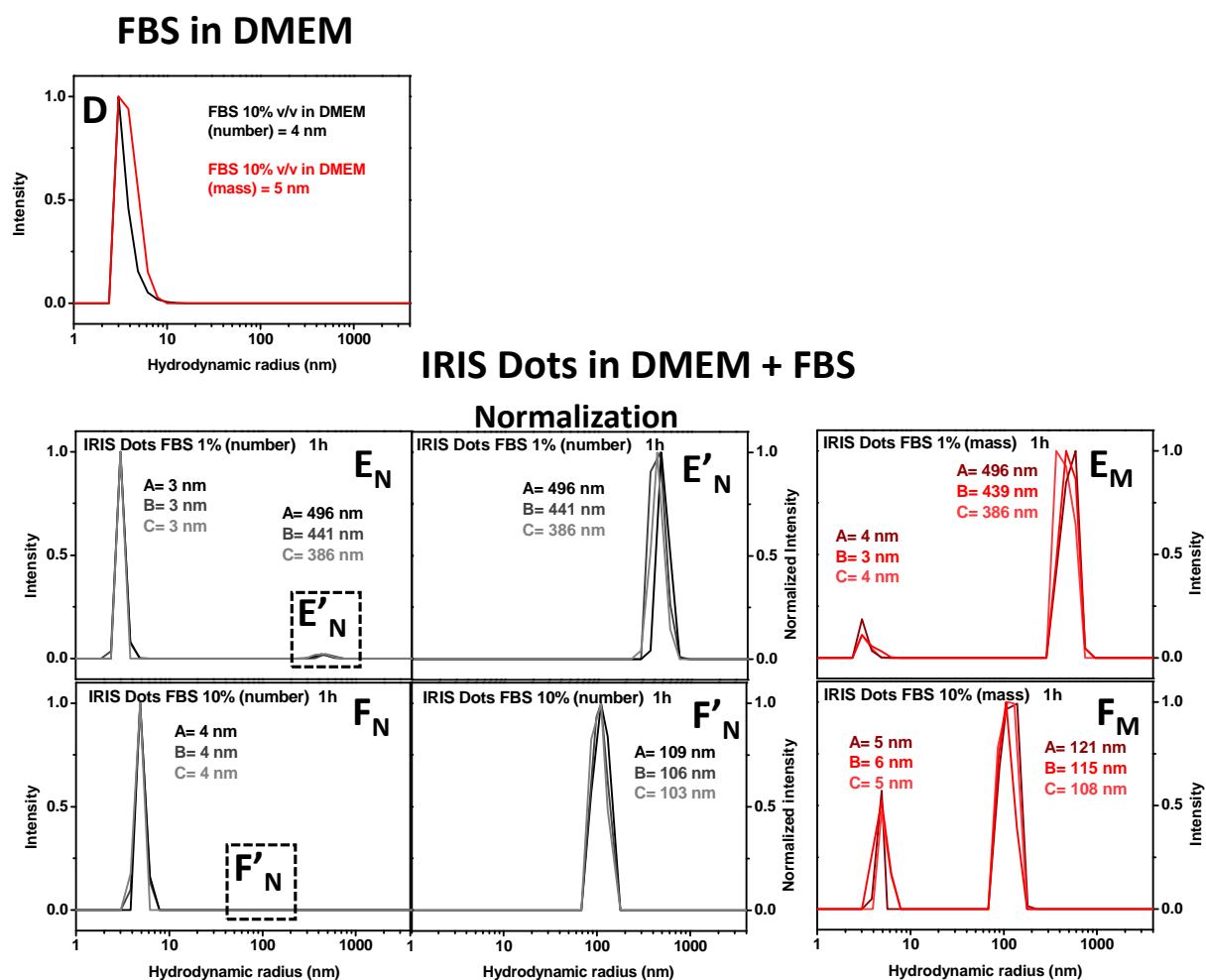


Figure S1, continued. Raw data of DLS measurements of FBS 10% v/v in DMEM (D) and IRIS Dots in DMEM in equilibrium with FBS proteins (E, F). Given the prevalence, in the number distributions, of the signal related to the presence of proteins in solution ($R_H = \text{ca. } 4\text{-}6$ nm), significantly more intense than the signal due to NP agglomerates, number distributions dealing with NP were normalized as reported in E' and F' panels.

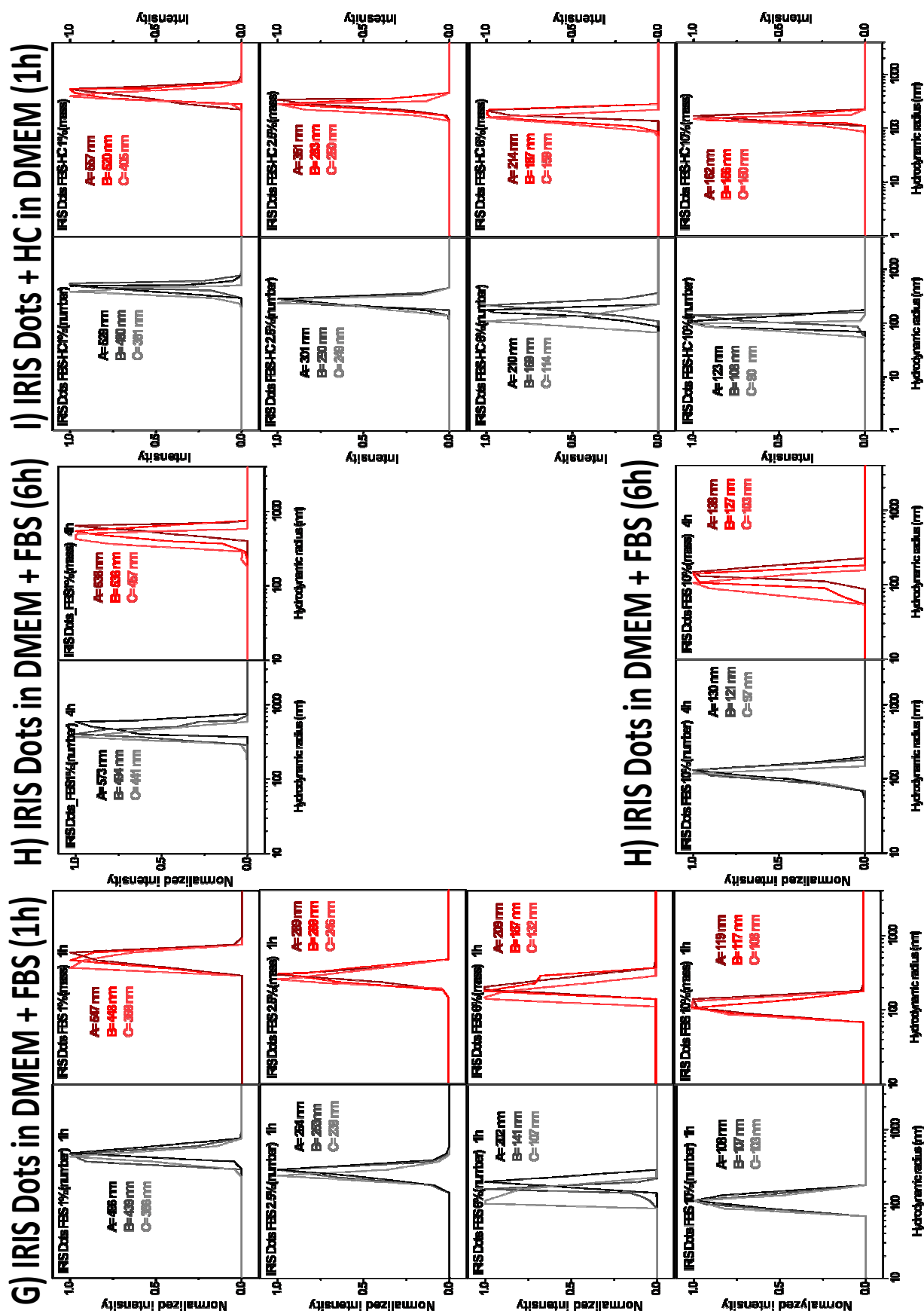


Figure S1, *continued*. Raw data of DLS measurements of IRIS Dots suspended in DMEM in presence of FBS after 1 and 6h of incubation (G and H respectively) and resuspended in DMEM in absence of FBS after removal of non adsorbed proteins through centrifugation cycles (I).

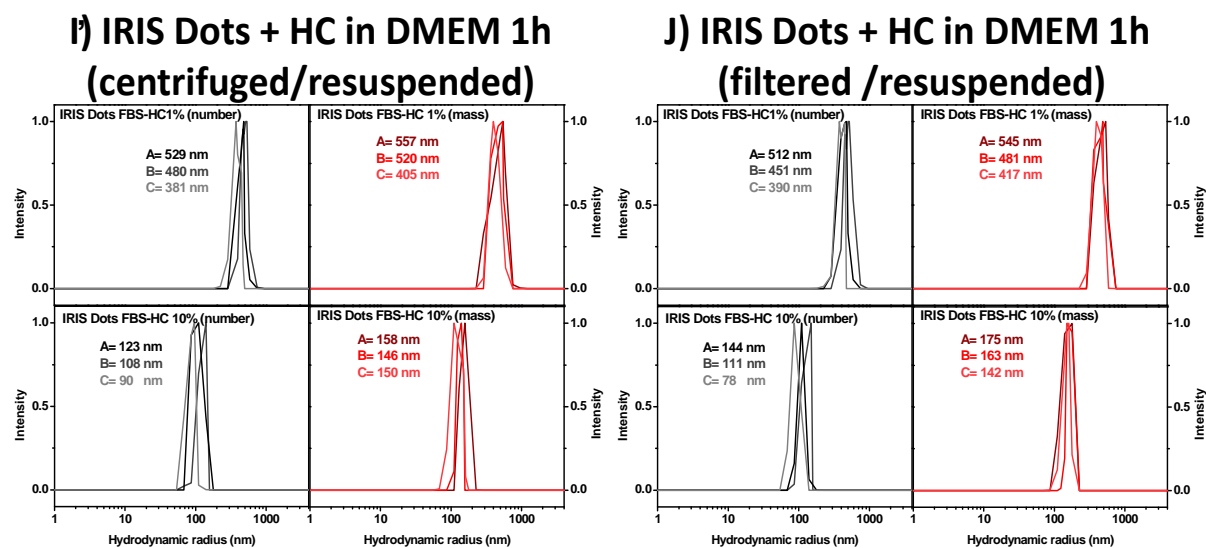


Figure S1, continued. Raw data of DLS measurements of IRIS Dots resuspended in bare DMEM after 1h of incubation with FBS 1 and 10% v/v and removal of non adsorbed proteins through centrifugation or filtration cycles (I and J respectively; data in panel I are a part of the results reported in the previous panel I).

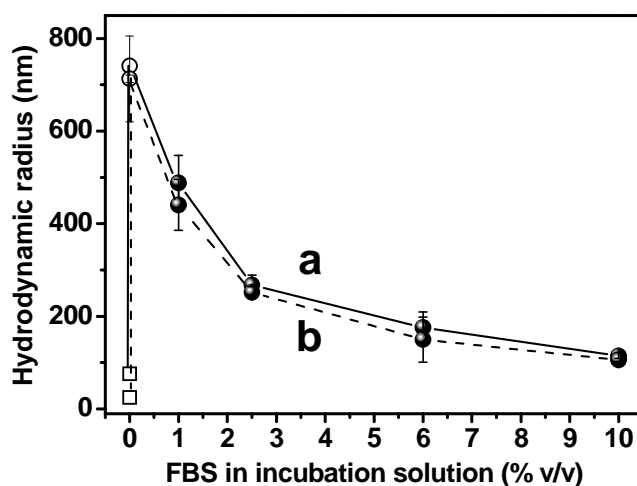
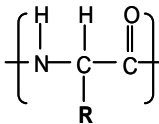


Figure S1, continued. Mean values of hydrodynamic radii reported in previous sections A, B and G, dealing with IRIS Dots suspended for 1h in distilled water (squares), DMEM (empty circles) and DMEM with different FBS concentrations (full symbols). Curves a) and b) refer to values resulting from mass and number distributions, respectively.

Table S1. *Section A:* mean hydrodynamic radii values of IRIS Dots in water and IRIS Dots suspended in DMEM for 1 and 6 hours. *Section B:* mean hydrodynamic radii of IRIS Dots suspended in DMEM in presence of FBS after 1 and 6h of incubation (column 2 and 3 respectively) and resuspended in DMEM in absence of FBS after removal of non adsorbed proteins through centrifugation or filtration cycles (column 4 and 5 respectively).

<i>Section A</i>		Mass (R_H; nm)		Number (R_H; nm)					
NPs/H₂O		75±11.8		25±00.0					
NPs/DMEM 1h		740±92.2		691±56.9					
NPs/DMEM 6h		755±68.5		706±39.6					
<i>Section B</i>		NPs+FBS 1h		NPs+FBS 6h		NPs+HC 1h		NPs+HC 1h(filtered)	
		<i>Mass</i>	<i>Number</i>	<i>Mass</i>	<i>Number</i>	<i>Mass</i>	<i>Number</i>	<i>Mass</i>	<i>Number</i>
1% FBS		488±52.2	441±55.0	544±90.7	503±66.4	494±79.3	463±75.4	481±64.4	452±66.3
2.5% FBS		268±21.5	252±12.5			295±51.5	280±27.4		
6% FBS		176±39.7	150±48.1			187±28.0	164±48.1		
10% FBS		115±6.1	106±3.5	123±17.9	116±17.1	144±15.0	107±16.5	160±16.7	111±38.0

Table S2. Database for the calculation of the amount of adsorbed peptide units per nm².
Section A. Data related to the average amino acid composition of adsorbed proteins. Data in column D were used as inputs (denominator) for the algorithm reported below.

Amino acid residue		A	B	C	D
entry		Amino acid residue mass [Dalton] ^a	Amino acid residue mass [μg, ×10 ¹⁶]	Amino acid residue relative abundance ^b	Amino acid residue relative mass [μg; ×10 ⁻¹⁷]
1	Tryptophan	186.20	3.09	0.012	0.37
2	Glycin	57.00	9.46	0.068	0.64
3	Alanine	71.10	1.18	0.076	0.90
4	Valine	99.10	1.64	0.066	1.09
5	Leucine	113.30	1.88	0.095	1.79
6	Isoleucine	113.20	1.88	0.058	1.09
7	Methionine	131.20	2.18	0.024	0.52
8	Proline	97.10	1.61	0.050	0.81
9	Phenylalanine	147.20	2.43	0.041	1.00
10	Serine	87.10	1.45	0.071	1.03
11	Threonine	101.10	1.68	0.056	0.94
12	Asparagine	114.10	1.89	0.043	0.81
13	Glutamine	128.10	2.13	0.039	0.83
14	Tyrosine	163.20	2.71	0.032	0.87
15	Cysteine	103.10	1.71	0.016	0.27
16	Lysine	128.20	2.13	0.060	1.28
17	Arginine	156.20	2.59	0.052	1.35
18	Histidine	137.10	2.27	0.022	0.50
19	Aspartic acid	115.10	1.91	0.052	0.99
20	Glutamic acid	129.10	2.14	0.065	1.39

^a)from: A.L. Burlingame, S.A. Carr, *Mass Spectrometry in the Biological Sciences*, Umana Press, Totowa, NJ, USA 1996; ^b)from: G. Trinquier, Y.-H. Sanejouand, *Protein Engineering* 1998, 11, 153–169.

Section B. Data related to the calculation of the amount of irreversibly adsorbed proteins on IRIS Dots agglomerates. Data in column D were used as inputs (numerator) for the algorithm reported below.

A	B	C	D
FBS concentration [%v/v]	Mass of irreversibly adsorbed FBS per unit mass of IRIS Dots [μg (FBS)-mg ⁻¹ (IRIS Dots)] ^a	Assumed Specific Surface Area for IRIS Dots agglomerates, SSA _{agg} [nm ² -mg ⁻¹] ^b	Mass of irreversibly adsorbed FBS per unit surface of IRIS Dots agglomerates [μg-nm ²]
1.0	45±10.8	0.39×1.0 ¹⁴	0.97×1.0 ⁻¹⁴
2.5	91±5.6	0.76×1.0 ¹⁴	1.21×1.0 ⁻¹⁴
6.0	195±29.7	1.22×1.0 ¹⁴	1.67×1.0 ⁻¹⁴
10.0	236±32.5	2.05 ×1.0 ¹⁴	1.23×1.0 ⁻¹⁴

^a)from TGA measurements; ^b) from Table 1 in the main text

The following algorithm was used for the calculation of the estimated amount of peptide units per nm² of the surface of IRIS Dots agglomerates:

$$\sum_{i=1}^{20} = \frac{\text{protein hard corona mass per nm}^2 \text{ of surface of IRIS Dots agglomerates } (\mu\text{g}\cdot\text{nm}^2; \text{ values in column D, section B})}{\text{value (i) of amino acid residue relative mass } (\mu\text{g}; \text{ values in column D, section A})} = \text{number of peptide units per nm}^2 \text{ of the surface of IRIS Dots agglomerates}$$

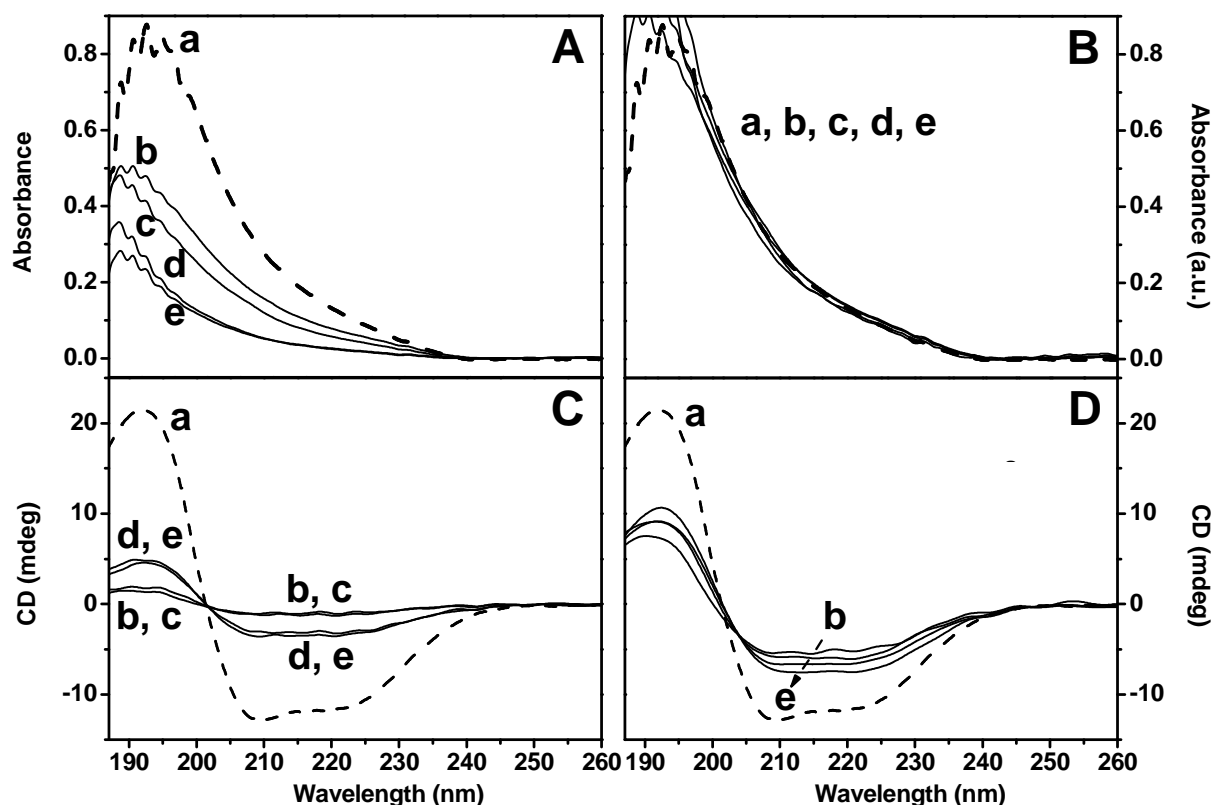


Figure S2. Absorbance (panels A, B) and CD-UV (panels C, D) spectra FBS in solution (dotted lines), and irreversibly adsorbed (protein hard corona) on IRIS Dots after incubation in DMEM with 1.0, 2.5, 6.0 and 10.0% v/v FBS (curves b, c, d and e, respectively), centrifugation/washing cycles. After the last centrifugation nanoparticles were suspended in distilled water, to attain a proper transparency in the spectral range investigated.

Comment to the figure

Suspensions of agglomerates of IRIS Dots carrying the protein hard corona were prepared by controlling the amount of sample in order to attain the same nominal concentration of proteins in unit volume of the samples. The amount of protein hard corona per mass of IRIS Dots obtained by TGA measurements and the mass of IRIS Dots used for the incubation with FBS solutions were used as data base. Despite the nominal equivalency of the amount of FBS proteins present in such samples, significant differences were obtained in the intensity of the absorption signal in the 180-260 nm range due to $\pi \rightarrow \pi^*$ and $n \rightarrow \pi^*$ transitions of the carbonylic groups in the polypeptide backbone (panel A). In particular, an opposite trend of the spectral intensities (decreasing from curve b to curve e) with respect the amount of adsorbed proteins per mass of IRIS Dots (increasing from curve b to curve e) was obtained. Likely, the origin of such discrepancy was the inhomogeneity of the suspension of the samples during the measurements. Thus, the Absorbance spectra were normalized to a common intensity value (panel B), and the normalization factors were used for the normalization of the corresponding CD-UV spectra (panel C: original; panel D: normalized). Finally, it is worth to notice that such data elaboration did not affect the shape of the CD-UV lines, and then the information contained in the change of the relative intensity of the negative bands at 209 and 219 nm with respect FBS in solution (see comments on Figure 3 in the main text).

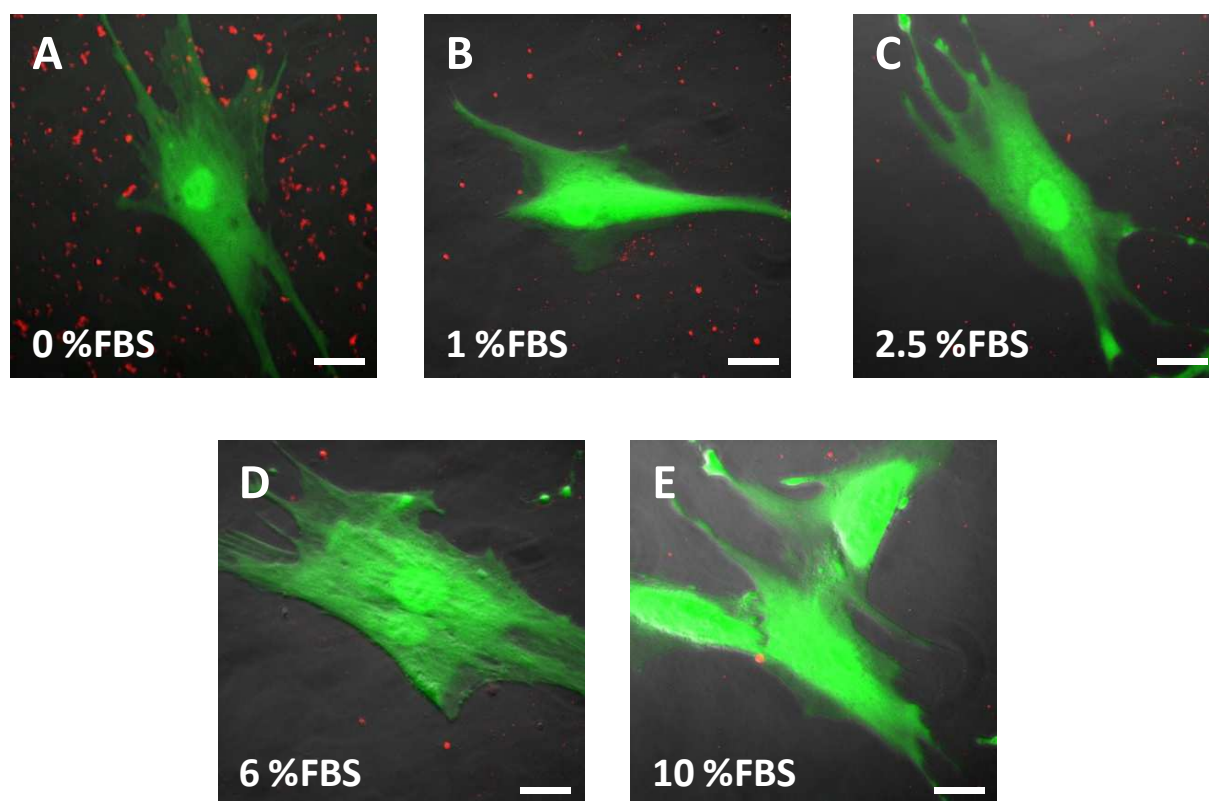


Figure S3. Confocal microscopy images of hMSCs after 1 h of incubation with $20 \mu\text{g mL}^{-1}$ IRIS Dots in bare DMEM (A) and different DMEM added serum conditions: 1.0% (B) 2.5% (C) 6.0% (D) and 10.0% (E) v/v. Cells were co-labeled with green 5-Chloromethylfluorescein Diacetate (CMFDA) $5 \mu\text{M}$. The white bar represents $20 \mu\text{m}$.

Table S3. Mean area of the NP aggregates observed in cellular environment at different FBS concentrations as analyzed with the ImageJ Plug-in “Analyze Particles” software.

FBS concentration [%v/v]	Mean area of NPs aggregates [μm^2]
0.0	0.412
1.0	0.056
2.5	0.045
6.0	0.033
10.0	0.032

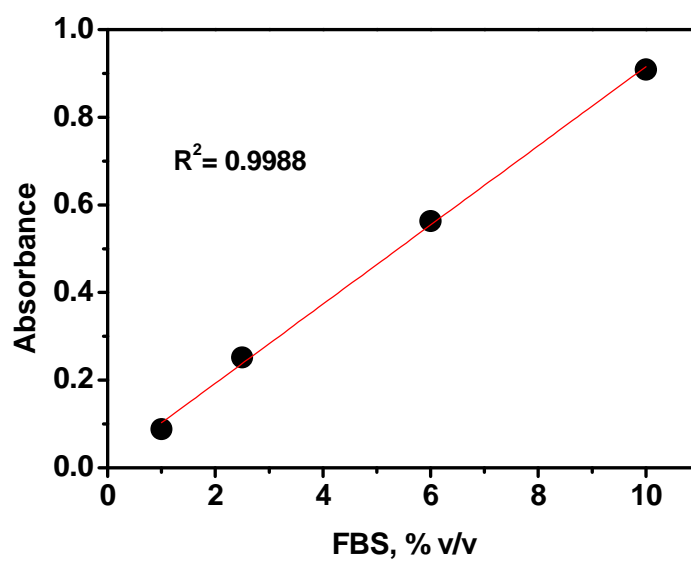


Figure S4. Calibration curve of Absorbances measured at $\lambda=280$ nm vs FBS concentration on serum incubation solutions (1.0, 2.5, 6 and 10% v/v).